Generation of transmission wave with low AM noise for sub-GHz CW-EPR spectrometer

Hideo Sato-Akaba[a*], Tsukasa Sakai[a], Hiroshi Hirata[b],

[a] Department of Systems Innovation, Graduate School of engineering Science, Osaka University, 1-3 Machikaneyama-cho, Toyonaka, Osaka 560-8531, JAPAN

[b] Division of Bioengineering and Bioinformatics, Faculty of Information Science and Technology, Hokkaido University, North 14, West 9, Kita-ku, Sapporo 060-0814, Japan

* Corresponding author: Hideo Sato-Akaba, Ph.D.

Department of Systems Innovation, Graduate School of engineering Science, Osaka University, 1-3 Machikaneyama-cho, Toyonaka, Osaka 560-8531, JAPAN

Phone: +81-6-6850-6313, Fax: +81-6-6850-6312, E-mail: akaba@ee.es.osaka-u.ac.jp

Keywords: Transmission power amplifier, AM noise, PM noise, digital EPR, *in vivo* EPR

Abstract

This study describes a technique to clean amplitude modulation (AM) noise of RF transmission waves, which is used to observe the sub-GHz CW-EPR spectrum. An RF transmitter amplifier that has the function of cleaning AM noise has been developed. Cleaning of the AM noise was owing to saturation of the output at the amplifier. Three stages of the amplifiers in series could effectively suppress the AM noise to about –176 dBc/Hz and –183 dBc/Hz at offset frequency of 10 kHz and 100 kHz, respectively at the carrier frequency of 750 MHz and the output power of 29 dBm. Since phase modulation (PM) noise is suppressed by phase sensitive detection, the AM noise in the transmission is dominant cause of the noise in the sub-GHz CW-EPR absorption spectrum using a reflection bridge, which depends on the quality factor of the resonator and the power of the RF transmission. The additive phase modulation (PM) noise of this amplifier was –171 dBc/Hz at an offset frequency of 100 kHz, which indicated that the frequency modulation (FM) of the transmission wave was not distorted with this amplifier. Therefore, conventional CW-EPR spectrometers that typically require FM for automatic frequency control or automatic tunning control can use this technique to increase sensitivity.

1 Introduction

Sub-GHz CW-EPR is mainly used for small animal applications where frequencies in the GHz band are undesirable due to dielectric loss in biological samples [1,2]. However, weak EPR signal intensity due to low EPR frequency and low Q factor of the resonator become a problem for the applications such as in-vivo EPR measurements. Therefore, developing a system that can measure EPR signals with high sensitivity is essential. Improving the signal-to-noise ratio (SNR) requires increasing signal intensity or decreasing noise of the measurement system. To increase the signal intensity, it is necessary to increase B_1 generated in the resonator by increasing the RF transmission power, or to use a resonator with a high Q factor. However, to reduce the noise in the EPR spectrum, the noise figure (NF) of the receiver circuit and the noise in the transmission wave must be reduced. In this research, we aim to increase the sensitivity by increasing the transmission power and reducing the noise in the transmission wave.

Noise of the RF transmission wave is mainly classified into amplitude modulation (AM) noise and phase modulation (PM) noise. AM noise is noise that modulates the amplitude of the carrier wave. When phase sensitive detection (PSD) is performed, noise appears in the same phase as the carrier wave. On the other hand, phase noise is noise that modulates the frequency of the carrier wave. When PSD is performed, it appears as noise with a phase that differs by 90 degrees from the carrier wave.

Magnetization generated by EPR resonance has absorption and dispersion components. This magnetization changes the inductance of the coil that is part of an LCR resonator. As a result, the impedance of the resonant circuit changes, which changes the reflection wave from the resonator. The reflection wave is effectively measured with a reflection bridge. An RF circulator or directional coupler is typically used in the reflection bridge to separate the reflection wave from the transmission wave. The isolation of these components is generally around 20 dB, so that leakage transmission signal become a problem for the receiver circuit. To solve this problem, the impedance mismatch in the resonator can generate a reflection wave in the resonator that cancels out the leaked transmission wave [3,4]. The reflection coefficient around the resonant frequency of the resonator changes as a function of the frequency. The transmission wave at the resonant frequency is suppressed more than the side band noise, so that reflected side band noise is relatively enhanced and degrade noise property of the reflection wave which is not related with EPR phenomenon. If the amplitude of the reflection coefficients for the upper and lower sidebands are different, then the AM to PM and PM to AM noise conversion may occur [5,6].

The reflection wave due to the magnetization of the absorption component has the same phase as the transmission wave, so it is affected by the AM noise of the transmission wave. On the other hand, the reflection wave due to the magnetization of the dispersion component has a phase difference of 90 degrees from the transmission wave. The generated noise due to the phase noise of the transmission wave at the resonator effect on the noise in dispersion spectrum [7,8]. When the noise originated from the AM noise of the transmission wave is larger than the thermal noise generated from the receiver circuit, it appears as noise in the absorption spectrum. Therefore, we propose and manufacture a transmission power amplifier that reduces the AM noise of the transmission wave rather than the PM noise. Analysis of noise in EPR spectra was performed using a digital EPR spectrometer. However, since common EPR spectrometers use analog PSD, we conducted a simple experiment using an analog spectrometer to demonstrate the noise reduction potential of the proposed amplifier.

2 Methods

2.1 Design

Reduction of AM noise in the transmission wave is performed by inserting the original transmission wave into the power amplifier at a power that saturates the amplifier [9,10]. Since this amplifier is intended to be used in the saturated region, it is called a saturated power amplifier (SPA). The shape of the wave after amplification is clipped due to output saturation, which removes AM noise but adds higher harmonic waves. However, the higher harmonic waves can be cleaned by inserting low-pass filters. A transmission amplifier circuit with three amplifying stages is designed to suppress the AM noise and increase output power.

Fig. 1 shows a schematic diagram of the developed amplifier. Commercial RF amplifier IC (Gali-06, Mini-Circuits) was used for the first and second-stage amplifiers because it was made of heterojunction bipolar transistors (HBT) with low additive PM noise. The typical additive PM noise level of this IC was reported as -171 dBc/Hz at 100 kHz offset from the carrier frequency of 2 GHz. In the final stage, four RF amplifier ICs (PHA-13HLN+, Mini-Circuits) were connected in parallel to increase the 1dB compression point (P1dB) and to decrease the contribution of noise generated in the amplifier ICs [11]. When driven by 8 V, the typical P1dB and NF values were 27.4 dB and 1.4 dB at 1GHz, respectively. The driving voltage was set at 4.8 V to reduce noise and heat generation in the final stage, yielding approximately 29 dBm over a frequency range of 700-850 MHz. Paralleling of amplifiers was performed using 90° hybrids (X3C07P1-03S, Anaren). This type of design is called a balanced amplifier and can protect against short or open output ports. After each amplifier IC, a low pass filter (LP0805H0750ASTR, KYOCERA AVX) or band-pass fitter (LDB15829AAD1A030, Murata Electronics) was inserted to eliminate higher harmonic waves. RF amplifier ICs used to build the SPA were summarized in Table 1.

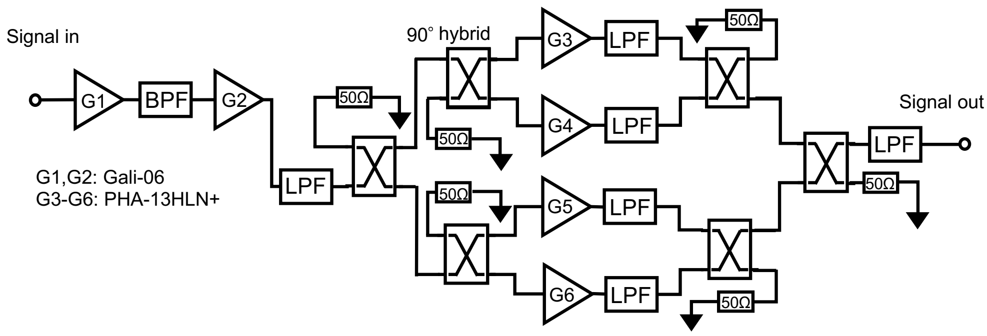

Fig.1 Schematic diagram of a saturated power amplifier (SPA) with three amplifier stages.

Table. 1 Performance[a] required for RF amplifier IC selection to use for RF sources B and C, SPA and PA

Product name	Technology	Frequency range (GHz)	Maximum input power (dBm)	Additive phase noise 100kHz offset (dBc/Hz)	NF (dB)	P1dB (dBm)	Gain (dB)
PHA-13HLN+	E-PHEMT	0.1 - 1	11 dBm		1.4 (1 GHz)	27.4 (1GHz)	20.4(1GHz)
HMC589AST89E	InGaP HBT	DC - 4	10 dBm	-176 (2GHz)	4.0 (DC-4GHz)	19 (0.5-1GHz)	21(DC-1GHz)
Gali-06	InGaP HBT	DC - 4	20 dBm	-171 (2GHz)	4.5 (1 GHz)	18.2 (1GHz)	12.2(1GHz)

a: Typical performance for each RF amplifier IC was obtained from the manufacturer's datasheet and homepage.

2.2 RF signal source

RF signal sources with different AM noise and PM noise were used to generate a transmission wave to investigate the functionality of the SPA and effectiveness of the SPA in EPR measurements. Specification of the RF sources are as summarized in Table. 2. An RF signal source A was a commercial RF synthesizer (N5172B, Keysight Technologies). The RF signal source A was used for the majority of the measurements because detailed RF frequency and RF power settings were possible. In some experiments, an additional locally constructed amplifier made from 8 RF amplifier IC (PHA-13HLN+) connected in parallel (PA) was used to increase RF power up to 28 dBm while preserving AM noise in the transmission wave. In addition, AM noise at 750 MHz and 100 kHz offset frequency changed from –149 dBc/Hz when automatic leveling control (ALC) was turned off to -135 dBc/Hz when ALC was turned on, which is useful to investigate the contribution of AM noise to the noise in the EPR absorption spectrum. The RF signal source B was a commercial PLL-based RF clock generator (PLL83B, Denshiken Co., Ltd.). The RF power increased up to 18 dBm after adding an RF amplifier IC (HMC589AST89E, Analog Devices). The PM noise of the RF signal source B was –125 dBc/Hz at 100 kHz offset frequency, while the AM noise was –159 dBc/Hz. RF signal source C was a locally constructed fixed frequency oscillator that generated a 750 MHz signal. The RF signal source C consisted mainly of a 1GHz SAW oscillator (CCSO-914X, Crystek Corp.), an x3 frequency multiplier (ZX90-3-452-S+, Mini-Circuits), a 1/4 prescaler (HMC905LP3E, Analog Devices), and an RF amplifier (HMC589AST89E) as shown in Fig. 2. The PM noise and AM noise at an offset frequency of 100 kHz were –161 dBc/Hz and –177 dBc/Hz, respectively. The use of the 1/4 prescaler, which generated a rectangular wave and then suppressed AM noise, was one of the reasons for the low AM noise level. The output power was 18 dBm using the final amplifier (HMC589AST89E). The RF signal source D was a commercial RF synthesizer (E8257D, Keysight Technologies), which was only used for the analogue EPR measurement. According to the datasheet, typical PM noise level at 100kHz offset in the frequency band of 500 MHz to 1000 MHz for the RF synthesizer were –135 dBc/Hz. RF amplifier ICs used for the RF sources B and C were summarized in Table 1.

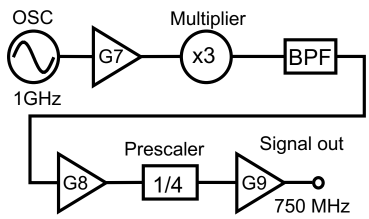

Fig. 2 Schematic diagram of an RF signal source C. Three RF amplifier ICs were used: G7-G8 (Gali-06) and G9 (HMC589AST89E).

Table. 2 Specifications of RF sources used for the measurement.

RF source	Type of the sources	Model	Noise without SPA[a]		Noise with SPA[a]	
			AM (dBc/Hz)	PM (dBc/Hz)	AM (dBc/Hz)	PM (dBc/Hz)
A	RF synthesizer	N5172B	-149 (ALC OFF)	-125	-183	-125
A'	RF synthesizer	N5172B	-135 (ALC ON)	-125	-183	-125
B	PLL-based clock generator	PLL83B	-159	-125	-183	-125
C	SAW based oscillator		-177	-161	-183	-161
D[c]	RF synthesizer	E8257D		-135[b]		

a: Values measured at 100 kHz offset for 750 MHz

b: Typical value at 100 kHz offset for 500-1000MHz from manufacture datasheet

c: RF source D was only used for the analog EPR spectrometer.

2.3 AM noise and PM noise measurements

The absolute PM and AM noises of the transmission wave were measured with a commercial RF phase noise analyzer (HA7062C, Holzworth Instrumentation Inc.). The

PM noise of the transmission wave is measured by PSD using a clean reference signal generated in the phase analyzer. On the other hand, AM noise measurements typically use diodes to detect the amplitude of the transmission wave. The output signal from a device under test (DUT) was filtered with a band-pass filter (ZX75BP-750-S+, Mini-Circuits) to eliminate low-frequency noises, which were sometimes observed in the noise spectrum. In the case of the amplifier as a DUT, the input power to the phase noise analyzer was typically adjusted to be 15 – 20 dBm by using a fixed attenuator to ensure sufficient SNR of the measurement. The RF source A (N5172B) was mainly used to generate original transmission signals.

2.4 Additive PM noise measurement

Additive PM noise is a PM noise added by RF components. A smaller additive PM noise is preferred because the additional PM noise generates noise when the down conversion to the baseband signal is performed with the reference signal with the original PM noise. The additive PM noise measurement for the developed amplifier was performed with the configuration shown in Fig. 3. A mechanical phase shifter (MODEL 6709-2, Sage Laboratories Inc.) was adjusted to create a quadrature reference signal for two LO inputs in the phase noise analyzer. A small phase difference between the two channels was calibrated to less than 0.5 degrees by changing the cable length.

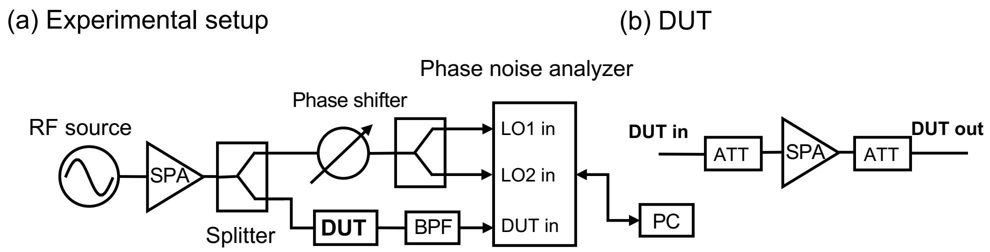

Fig.3 (a) Experimental setup for additive phase noise measurements: (b) A DUT setup for additive PM noise of the SPA.

2.5 Reduction of AM noise using RF amplifiers in saturation

AM noise reduction by an RF amp (Gali-06) was investigated by changing the intensity of the RF transmission wave inserted into the amplifier from –12 dBm to 18 dBm. A low pass filter (LP0805H0750ASTR) was inserted after the amplifier to remove the higher harmonic waves. The power of the RF transmission wave fed to the RF amp was adjusted using a variable attenuator (50DR-046, JFW Industries, Inc.). Subsequently, the relationship between the number of amplifiers connected in series and the reduction of AM noise was investigated. Furthermore, up to four RF amps (Gali-06) were connected in series. The same bias resistor and drive voltage were used for each amplifier.

2.6 EPR measurement

EPR measurements were performed using the previously reported sub-GHz digital CW-EPR spectrometer [4,12,13] and a homodyne analog CW-EPR spectrometer [14,15]. The primary distinction between digital EPR and analog EPR in this work was whether the phase-sensitive detection to separate the EPR absorption and dispersion spectra was performed using digital signal processing or analog circuitry [16–18]. Furthermore, in the control for suppressing the reflection wave from the resonator, the control signal differs depending on whether it is generated by digital signal processing or by an analog circuit. Since the conventional analog EPR was widely used to measure biological applications, we investigated whether the noise could be reduced using the SPA in analog EPR.

The digital EPR spectrometer mainly consisted of a digital EPR console, an RF reflection-type bridge, a compact arrayed magnet, and a voltage-controlled multi-loop-gap resonator with barium strontium titanate (BST) based tunable capacitors [3]. The size of the loop-gap part of the resonator was ϕ24 mm × 25 mm. Unloaded Q of the resonator was 480. A glass bottle containing 4 mL TEMPOL aqueous solution (1 mM) was used for the measurement. The measurement parameters were an RF frequency of 750 MHz, a magnetic modulation field of 0.1 mT, a magnetic field sweep width of 2 mT, and a scan time of 40 ms. The modulation frequency was set to 1/4096 of the ADC sampling frequency so that digital demodulation can be easily done on the PC[4]. The sampling frequency was set to 4/7 times the transmission RF frequency of 750 MHz, so the modulation frequency became 105 kHz. The passband of the digital band-pass filter was set at 4 kHz, which was applied before demodulation of the modulated EPR signal. To use external signal sources as a EPR transmission wave, the EPR digital console was modified to accept an external ADC clock signal. The ADC clock signal was generated from the EPR transmission wave by using a passive x4 frequency multiplier based on a step recovery diode (MAVR-044769-12790T, MACOM) and a band-pass filter (CER0535B, CTS Electronic Components).

The analog EPR spectrometer mainly consisted of a commercial RF synthesizer (E8257D), an RF reflection-type bridge, a parament EPR magnet (26.8 mT, X-5253, Neomax Company, Hitachi Metals, Ltd.), a lock-in amplifier, a DAQ board (PCIe-6259, National Instruments), and a voltage-controlled multi-loop-gap resonator with varactor diodes [19]. The size of the loop-gap part of the resonator was ϕ24 mm × 30 mm. Unloaded Q of the resonator was 551. A TEMPOL aqueous solution (1 mM) in a 1mL tube was used as a sample for the measurement. The measurement parameters were an

RF frequency of approximately 750 MHz, a magnetic modulation field of 0.1 mT, a magnetic field sweep width of 6 mT, and a scan time of 100 ms. The noise on the baseline of the EPR spectrum was measured by changing the transmission power using fixed attenuators.

2.7 Noise measurement under EPR acquisition condition

It is necessary to know the correct phase to separate noise in absorption and dispersion modes. One of the methods is to measure isotropic EPR signal while changing the phase of the two quadrature baseband signals. This method is useful when the SNR of the EPR signal is good. If the SNR is poor, this method will not work properly. In this case, minimizing the noise will help to find the correct phase for absorption mode when the transmission noise contributes more than the thermal noise of the receiver circuit.

The noise in the EPR spectrum can be evaluated with the noise observed without magnetic field sweep and field modulation since magnetic resonance generally does not generate noise. The reflection signal from the resonator was fed into the digital EPR console after the receiver circuit to measure these noise spectra, as shown in Fig. 4. The signal fed to the EPR console was digitally down-converted into baseband quadrature signals in an FPGA IC. The one of the baseband signals after the phase correction was stored in the FPGA and transferred to the PC. The noise spectra were generated by fast Fourier transform (FFT) of the transferred data on the PC. EPR spectrum were also generated by digital PSD of the transferred data at the field modulation frequency.

The baseband signals became error signals for feedback control to increase isolation between the transmission and reception. Two error digital signals were converted into analog automatic tuning control (ATC) signal and automatic matching control (AMC) signal to change the capacitance in a voltage-controlled resonator[3,4]. The leakage wave at the circulator in the reflection bridge was canceled with the reflection from the resonator controlled by changing impedance of the resonator. This feedback approximately matched the resonant frequency of the resonator to the RF frequency of the transmission wave.

To investigate the effect of unloaded Q of the resonator on the noise spectra, glass bottles filled with different concentrations of NaCl aqueous solution (0.9%, 0.45%, and 0%) were prepared and inserted into the resonator. The unloaded Q of the resonator was 140, 190, and 350, which were measured with a network analyzer (MS2024B, Anritsu). The thermal noise spectrum of the receiver circuit, which is noise floor of the measurement, was also measured by terminating the connection of the circulator port from the resonator and disconnecting the connector for the transmission wave. The noise level when the receiver circuit was terminated with a 50 Ω resistor is set to 0 dB. The noise level in dispersion and absorption modes is expressed as an increase from the noise floor. The incident RF power changed from –4 dBm to 22 dBm for the digital EPR spectrometer.

For the analog EPR spectrometer, the absorption spectra were measured by changing the incident power from 1.4 dBm to 9.6 dBm. The noise level was evaluated using the portion where the EPR signals were not observed.

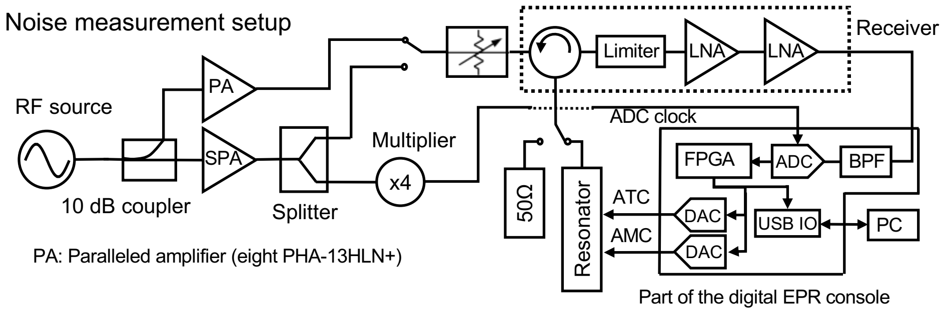

Fig.4 Experimental setup to measure noise in absorption and dispersion modes with and without the SPA. To increase the RF incident power up to 22 dBm without using the SPA, a parallel amplifier consisting of eight identical amplifier ICs, driven in the linear region, was used. Automatic tuning control (ATC) and automatic matching control (AMC) of the resonator were used to cancel RF leakage at the circulator with a reflection wave from the resonator.

3 Results and discussion

3.1 Cleaning of AM noise in the transmission waves

Fig. 5a shows the AM noise spectrum at different input powers to the RF amplifier (Gali-06), and Fig. 5b shows the noise spectrum with different numbers of the RF amplifiers in series. Figure 6 shows the output power of the amplifier as a function of the input power. The AM noise of the output signal gradually decreases as the input power increases and the output power begins to saturate. This can be explained by the clipping of the output due to saturation leading to loss of AM noise. When the input power was 18 dBm, AM noise of –179 dBc/Hz at 100 kHz offset frequency was obtained. However, the input of 18 dBm was relatively high to accept RF transmission waves from various RF signal sources. Additional identical amplifiers were tested in series to reduce the input power of the amplifier to about 10 dBm. The result is shown in Fig. 5b, indicating that two RF amplifier in series are enough to improve AM noise reduction. Because of the output signal saturation and the use of the identical amplifier in series, the power did not increase more than 16 dBm. Four medium-power RF amplifiers (PHA-13HLN+) connected in parallel were used as a third-stage RF amplifier to increase output power. The additional noise generated by each amplifier was uncorrelated; thus, parallelization doubled the noise. However, the transmission power increased 4 times. The result is a relative reduction in amplifier noise. Finally, the AM noise was reduced to -183 dBc/Hz at an offset frequency of 100 kHz, as shown in Fig. 7. This noise level showed almost the same level even when using the RF signal sources with different AM noise levels. The AM noise levels for the different RF sources were summarized in Table 2. For example, when the RF power was attenuated to 22 dBm, the AM noise was attenuated to –161 dBm/Hz, which is 16 dB higher than the thermal noise contribution of –177 dBm/Hz at room temperature.

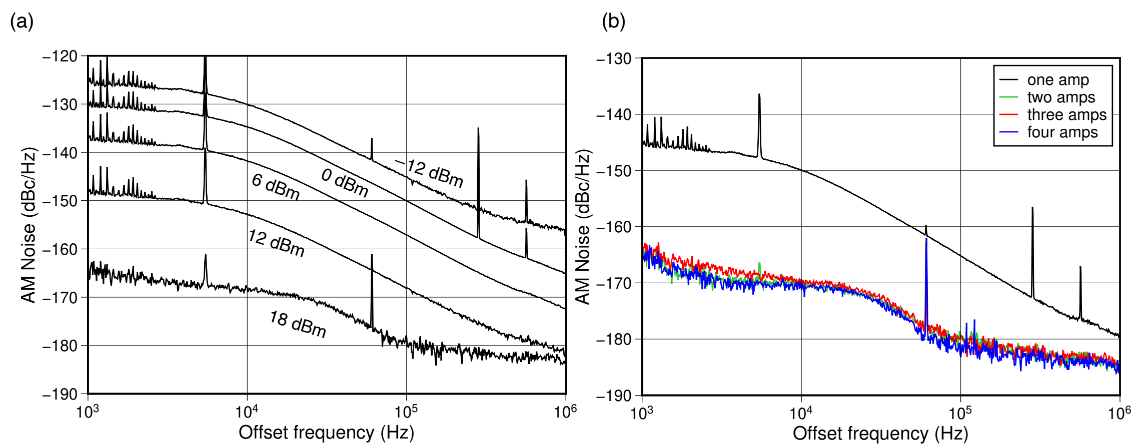

Fig. 5 AM noise spectra of amplified transmission waves generated from the RF source A: (a) different input power (–12 dBm to 18 dBm) using a single RF amplifier (Gali-06) and (b) fixed input power (10 dBm) using several amplifiers in series.

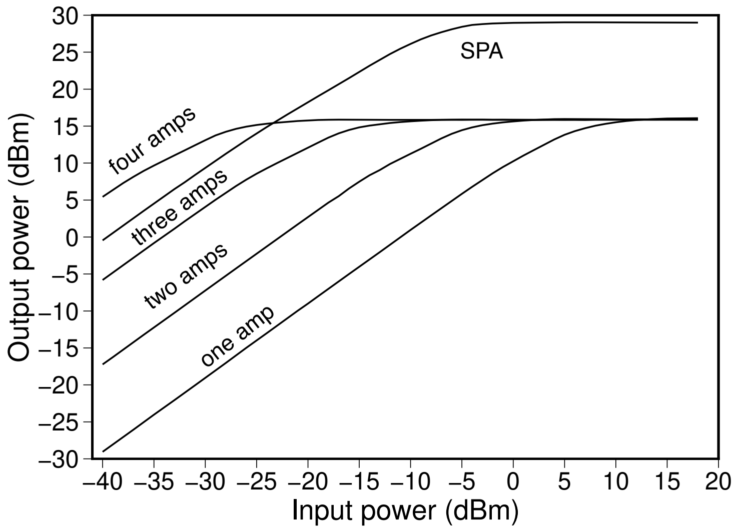

Fig. 6 Dependence of output power on the input power of the amplifiers in series. The

saturation power of the SPA is 13 dB higher than other amplifiers.

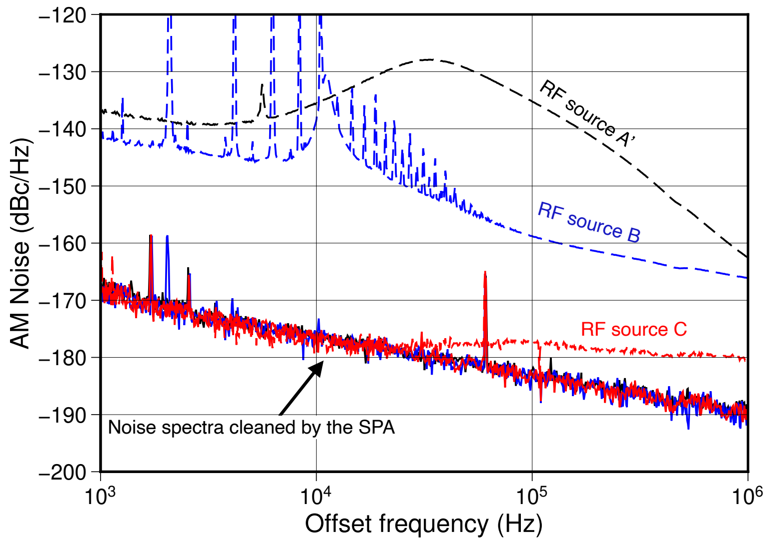

Fig. 7 Comparison of AM noise spectra from original transmission waves (dashed lines) and cleaned waves (solid lines) by the SPA. Curve colors indicate different RF sources.

3.2 Additive PM noise of the saturated power amplifier (SPA)

Fig. 8 shows the additive PM noise as an offset frequency function when the output of the amplifier is saturated. The absolute PM noise of the RF source C is also shown. Additive PM noise was found to be –171 dBc/Hz at 100 kHz, which was 10 dB smaller than the absolute PM noise. This amplifier did not affect the FM modulation of the transmission wave due to the small additive PM noise. Therefore, it could also be used for conventional EPR spectrometers that require FM modulation of transmission waves used for automatic frequency control and automatic tuning control.

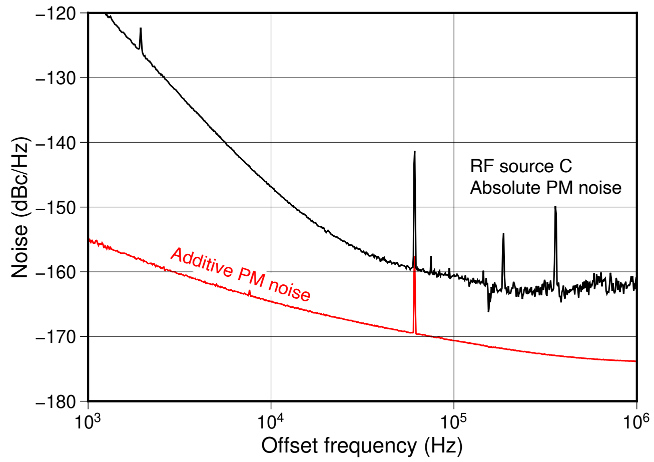

Fig. 8. Additive PM noise (red line) of the SPA measured with the RF source C. The

absolute PM noise (black line) of original transmission wave from the RF source C is also shown as a reference.

3.3 Noise under EPR acquisition condition

Fig. 9 shows the noise spectra observed using the digital EPR spectrometer with different RF signal sources except applying magnetic field sweep and field modulation. The noise spectra with either the maximum value (dispersion mode) or minimum value (absorption mode) after 100kHz were shown to have separate noise contributions, such as the PM and AM noises. The red dashed and solid curves expressed the noise spectra obtained without the SPA, while the black dashed and solid curves expressed those obtained with the SPA. The flat noise spectrum (shown in the blue line) was the noise floor of the receiver circuit, including the 50 Ω terminated circulator. Therefore, noise greater than the noise level of the receiver circuit was due to noise generated by the transmission wave fed into the resonator. The noise levels at 100 kHz offset were summarized in Table 3.

The large values in the noise spectra after 10 kHz offset were measured for dispersion mode with and without the SPA in Fig. 9. The difference between the values at 100 kHz offset in Figures 9a and 9f is 34 dB, which approximately corresponds to the difference in PM noise between RF source A (–125 dBc/Hz) and RF source C (–161 dBc/Hz) at 100 kHz offset. The reduction of the AM noise by the SPA did not impact on the noise for dispersion mode, which indicates that the AM to PM conversion noise was negligible. Therefore, the origin of this noise was due to the PM noise. The upper and lower sidebands of PM noise are attenuated and reflected in the antiphase by a reflection bridge, including a resonator acting as a band-stop filter. In addition, the transmission carrier is mostly removed. This worsens the phase noise of the reflection wave. The attenuated sideband noises remain in the baseband signals after PSD and are detected as noise because the PM noise of the reflection wave and the PM noise of the reference wave for the PSD are not identical.

The lower noise levels were measured for absorption mode with and without the SPA. As shown in Figures 9a and 9f, when using SPA, the phase noise of the transmission waves differed by 36 dB, but the noise levels in the absorption mode were similar. This indicates that the PM to AM conversion noise was negligible. Additionally, when using SPA, the AM noise levels of the transmission waves were reduced to -183dBc/Hz. This is why the noise levels in the absorption mode were similar.

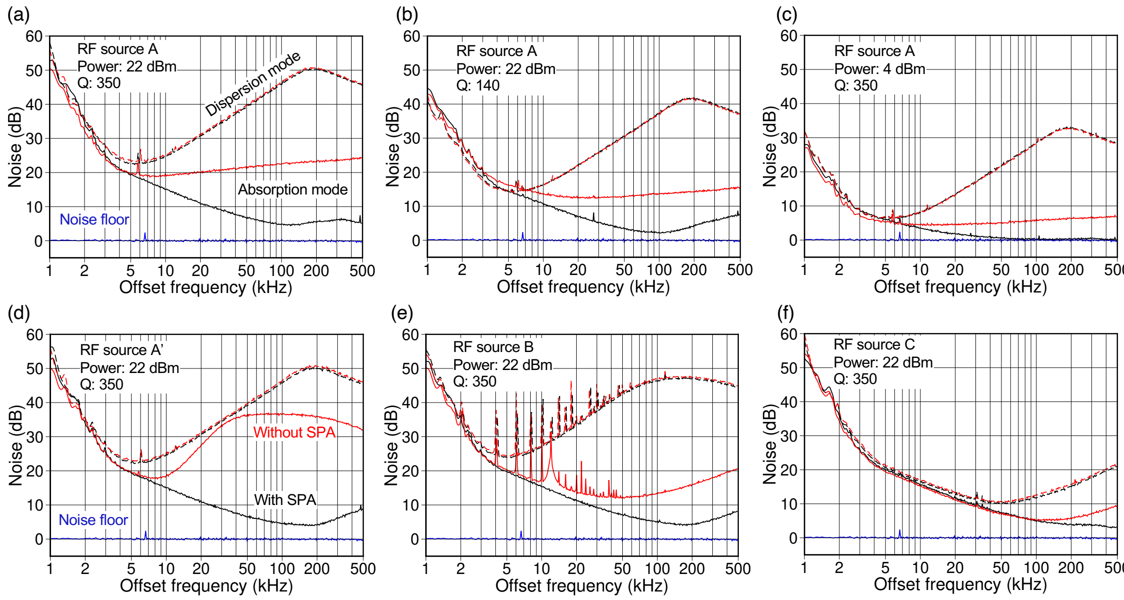

Fig. 9 Noise spectra in dispersion mode (dashed line) and absorption mode (solid line) with (black) and without (red) the SPA: (a) RF source A, RF incident power 22 dBm, Q of the resonator 350, (b) RF source A, 22 dBm, Q = 140, (c) RF source A, 4 dBm, Q = 350, (d) RF source A', 22 dBm, Q = 350, (e) RF source B, 22 dBm, Q = 350, and (f) RF source C, 22 dBm, Q = 350. Noise floor of the receiver circuit was shown in blue. The noise spectra were acquired with the digital EPR spectrometer.

Table. 3 Summary of the noise levels in absorption and dispersion modes at 100 kHz offset.

Measurement condition					Result of the noise (dB)[a]	
RF source	Power (dBm)	AM noise (dBc/Hz)	PM noise (dBc/Hz)	Q of the resonator	Abs. (SPA)[b]	Disp. (SPA)[b]
A	22	-149	-125	350	22.5 (4.6)	46.2(46.0)
A	22	-149	-125	140	13.6(2.1)	37.4(37.4)
A	4	-149	-125	350	5.7(0.2)	28.5 (28.6)
A'	22	-135	-125	350	36.5(4.6)	46.2(45.7)
B	22	-159	-125	350	13.4(5.0)	46.9(46.4)
C	22	-177	-161	350	5.2(5.1)	12.4(12.0)

a: The noise level when the receiver circuit was terminated with a 50 Ω resistor was set to 0 dB.

b: Results in parentheses were obtained using the SPA

The difference between noise in absorption and dispersion modes at 100 kHz offset for the original transmissions in Figs. 9a and 9d were 24 dB and 10 dB, respectively. This difference corresponded to the difference between PM noise and AM noise, indicating that the sideband contribution to the noise levels for absorption and dispersion modes was similar for PM and AM noise. Figure 10 plots the noise levels in absorption mode at 100 kHz offset as a function of the AM noise and the noise levels in dispersion mode as a function of PM noise. This results also show that the noise contributions to the EPR spectrum from the AM and PM noise of the transmission wave were nearly identical and appeared down to around -170 dBc/Hz at the RF incident power of 22 dBm and the resonator Q of 350.

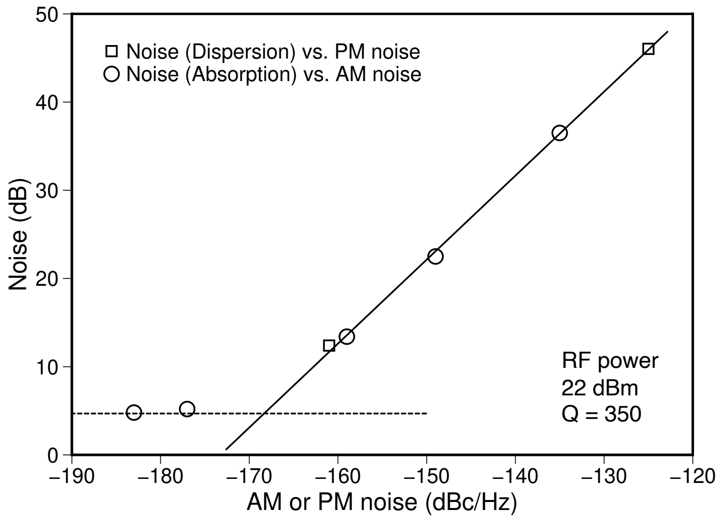

Fig. 10 Values of the noise spectra at 100 kHz offset plotted as a function of the transmission wave noise: (○) noise in the absorption mode vs. AM noise and (□) noise in the dispersion mode vs. PM noise. The incident RF power was 22 dBm. The solid line represents the contribution due to PM or AM noise of the transmission wave, and the dotted line represents the unknown contribution originating from the transmission wave.

If the PM and AM noises for the transmission wave were similar, similar noise levels in the absorption and dispersion EPR spectra should be observed. However, in the case of the noise in the absorption mode in Fig 9f, the noise level at 100 kHz was dominated by an unknown process. Therefore, further AM noise reduction of less than –177 dBc/Hz was not currently useful in our configuration of the digital EPR spectrometer. Moreover, finding the cause of that process as important as it resulted in further noise reduction.

The difference of the noise level at 100 kHz offset for with and without the SPA is enhancement of the SNR of the EPR absorption spectrum if the field modulation frequency is set at 100 kHz and the EPR signal is not saturated. When the Q of the resonator (Fig. 9b) or the power of the incident wave (Fig. 9c) was small, the SNR of the EPR spectra should decrease because the thermal noise of the receiver circuit limited the noise reduction due to the low Q or low incident power. As the Q of the resonator increases and the AM noise becomes larger compared to the thermal noise of the receiver circuit, the SNR of the absorption spectrum no longer increases. Therefore, reducing AM noise contributes to increasing SNR.

Fig. 11 shows the noise power spectral density at 105 kHz in the absorption mode as a function of the incident power to the resonator. The frequency 105 kHz was the magnetic field modulation frequency used in this digital EPR spectrometer, and digital PSD was performed at this frequency to obtain the ERP spectrum and evaluate the noise. The noise data was obtained with the transmission waves having different AM noise. The triangle, circle, and square marks expressed AM noise of –135 dBc/Hz, –152 dBc/Hz, and –177 dBc/Hz at 100 kHz offset, respectively. The noise level was normalized by the noise obtained when the circulator port was terminated to the resonator with 50 Ω resistor.

Noise data plotted as triangle marks in Fig. 11 can be fitted with a linear function. A slope coefficient of 1.0 indicates that the noise power is proportional to the incident power. This means that the noise contribution is dominated by AM noise. In this case, increasing the incident power does not improve the SNR because the noise voltage increases at the same rate as the EPR intensity. When the level of AM noise was getting smaller to -177 dBc/Hz, the thermal noise of the receiver circuit dominated in the noise below the incident power of 9 dBm. In this case, the increase in noise power is not proportional to the incident power such that the increase in incident power should improve the SNR. For example, if the transmission wave has AM noise of –152 dBc/Hz, approximately 15 dB SNR enhancement using the SPA should be achieved at the incident power of 21 dBm and Q of the resonator 350.

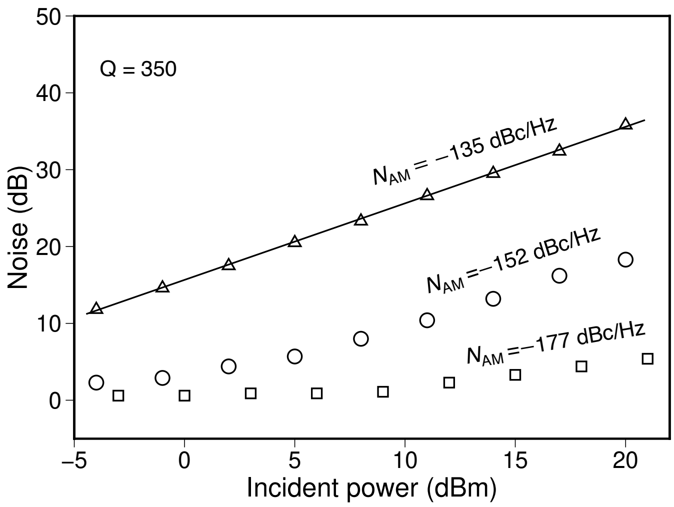

Fig. 11 Noise levels in the absorption mode at 105 kHz obtained with the transmission waves which had the different AM noise (N_{AM}): (△) AM noise of –135 dBc/Hz, (○) –152 dBc/Hz, and (□) –177 dBc/Hz at 100 kHz offset. The noise data were acquired with the EPR console under the EPR acquisition condition.

3.4 Comparison of EPR spectra with and without the SPA

Fig. 12 shows single scan spectra from TEMPOL aqueous solution acquired using transmission waves with different AM and PM noises with and without applying the SPA. The levels of the AM and PM noise for the RF sources at 100 kHz offset measured with the digital EPR spectrometer are shown in Table 1. The spectrum shown above in the figure was the absorption spectrum, while the spectrum shown below was the dispersion spectrum. The transmission power to the resonator was set to 22 dBm. AM noise was removed from the transmission wave, and noise in the absorption spectrum was reduced by inserting the SPA, as shown in Figs. 12d and 12e. Since the incident power was the same, the EPR signal intensity should be the same. Therefore, SNR was improved by reducing noise. However, because the SPA does not improve PM noise, as shown in Fig. 8, there was almost no change in noise in the dispersion spectrum. The AM noise appeared in the absorption spectra, while the PM noise appeared in the dispersion spectra. Hence, we confirmed that cleaning AM noise from the transmission wave was useful to increase SNR of the spectrum.

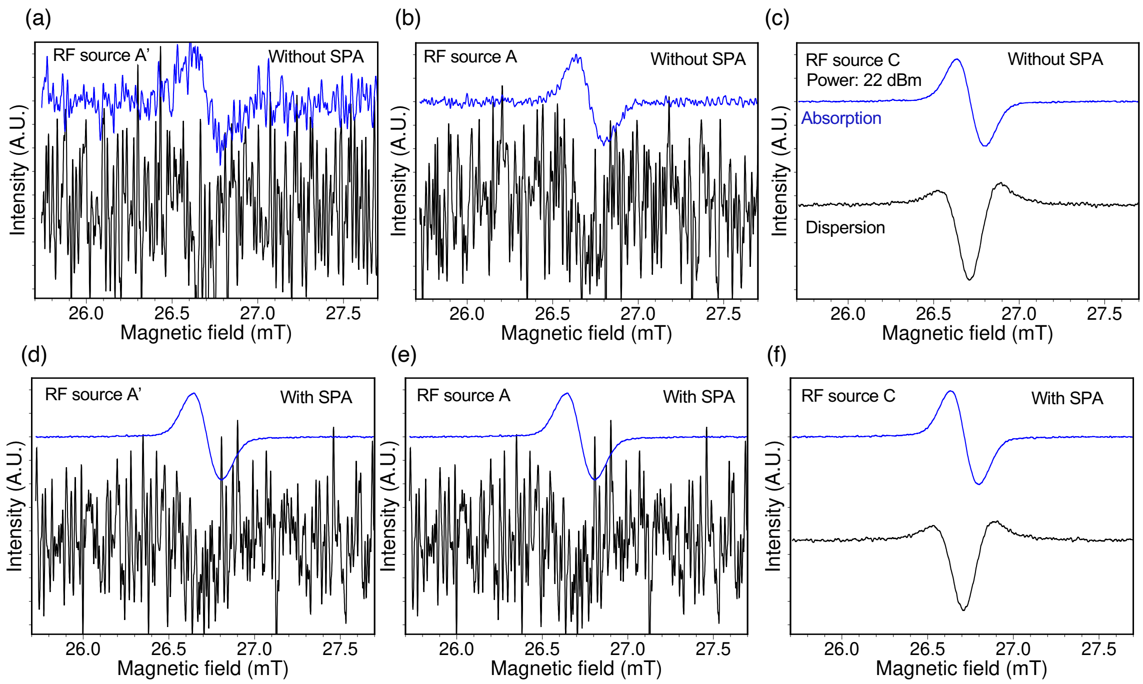

Fig. 12 Single scan EPR absorption (above) and dispersion (below) spectra from TEMPOL aqueous solution acquired with the digital EPR spectrometer. The incident RF power was set at 22 dBm, and different RF sources were used: (a) RF source A', (b) RF source A, (c) RF source C, (d) RF source A' and use of the SPA, (e) RF source A and use of the SPA, and (f) RF source C and use of the SPA.

Figures 13a and 13b show single scan absorption spectra from TEMPOL aqueous solution with a different incident power of approximately 1 dBm and 9 dBm, which were measured with the analog EPR spectrometer. The spectrum shown below was obtained using the SPA, while the spectrum shown above was obtained without the SPA. From the result, the higher the incident power the difference of the noise level becomes apparent. Figure 13c shows the noise dependence on the incident power with and without the SPA. A noise reduction of 8 dB was achieved with the incident power of 9 dBm.

Generally, the AM noise is smaller than the PM noise. Therefore, choosing the RF source with lower PM noise probably lower the AM noise. However, in normal applications where only absorption spectra are used, using the SPA eliminates the need for expensive oscillators with extremely low PM noise.

As the intensity of the transmission wave increases, the magnetic field generated within the resonator increases, and the signal increases. As the size of the resonator increases, the efficiency of magnetic field generation decreases. Therefore, if the object to be measured becomes larger, the transmission power must be increased. In such cases, reducing the AM noise of the transmission wave is important. Furthermore, in Rapid Scan CW-EPR, which can increase transmission power compared to conventional CW-EPR[20,21] , the reduction of AM noise in the transmission waves can be expected to improve SNR.

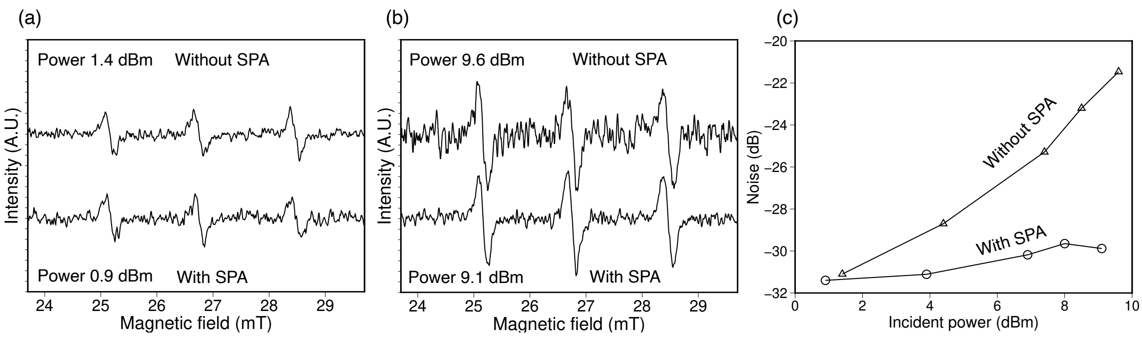

Fig. 13 Single scan EPR absorption spectra from TEMPOL aqueous solution acquired with the analog EPR spectrometer with and without using the SPA at different incident power (a) and (b). (c) The dependence of the noise in the EPR spectra on the incident power with and without the SPA.

4 Summary

In this study, the transmission wave's AM noise was reduced to less than -180 dBc/Hz at an offset frequency of 100 kHz and an output power of 29 dBm using a three-stage amplifier in saturation. The achieved level of the AM noise was almost independent of

RF sources. We confirmed that AM noise of the transmission wave could be the major noise source in the first derivative sub-GHz EPR absorption spectrum. This effect was larger for the high Q resonator and high RF power applied to the resonator. The additive PM noise of this amplifier was –171 dBc/Hz at the offset frequency of 100 kHz, indicating that the FM of the transmission wave was not distorted with this amplifier. Therefore, conventional CW-EPR spectrometers that typically require FM for automatic frequency control or automatic tunning control could use this technique to increase sensitivity.

Acknowledgment
This work was supported by JSPS KAKENHI Grant Number JP21H01341.

Reference

[1] L.J. Berliner, ed., In Vivo EPR (ESR), Springer US, Boston, MA, 2003. https://doi.org/10.1007/978-1-4615-0061-2.

[2] G.R. Eaton, S.S. Eaton, EPR Spectrometers at Frequencies Below X-band, in: L.J. Berliner, C.J. Bender (Eds.), EPR: Instrumental Methods, Springer US, Boston, MA, 2004: pp. 59–114. https://doi.org/10.1007/978-1-4419-8951-2_2.

[3] H. Sato-Akaba, M. Tseytlin, Development of an L-band rapid scan EPR digital console, Journal of Magnetic Resonance 304 (2019) 42–52. https://doi.org/10.1016/j.jmr.2019.05.003.

[4] H. Sato-Akaba, M.C. Emoto, H. Hirata, H.G. Fujii, Design and testing of a 750 MHz CW-EPR digital console for small animal imaging, Journal of Magnetic Resonance 284 (2017) 48–58. https://doi.org/10.1016/J.JMR.2017.09.008.

[5] Magnus Danielson, AM to PM conversion of linear filters, ArXiv:1805.07224 (2018).

[6] G Thirup, S Frydkjaer, A 0.5 μs time resolving superheterodyne ESR spectrometer, J Phys E 13 (1980) 1214. https://doi.org/10.1088/0022-3735/13/11/017.

[7] G.A. Rinard, R.W. Quine, B.T. Ghim, S.S. Eaton, G.R. Eaton, Easily Tunable Crossed-Loop (Bimodal) EPR Resonator, J Magn Reson A 122 (1996) 50–57. https://doi.org/10.1006/jmra.1996.0173.

[8] J.S. Hyde, R.A. Strangeway, J.W. Sidabras, Dispersion EPR: Considerations for Low-Frequency Experiments, Appl Magn Reson 53 (2022) 193–206. https://doi.org/10.1007/s00723-021-01352-z.

[9] N. Erikson, AM Noise in Drivers for Frequency Multiplied Local Oscillators, 15th International Symposium on Space Terahertz Technology (2004) 135–142.

[10] A. Hati, C.W. Nelson, D.A. Howe, Vibration-induced PM and AM noise in microwave components, IEEE Trans Ultrason Ferroelectr Freq Control 56 (2009) 2050–2059.

https://doi.org/10.1109/TUFFC.2009.1288.
[11] R. Boudot, E. Rubiola, Phase noise in RF and microwave amplifiers, IEEE Trans Ultrason Ferroelectr Freq Control 59 (2012) 2613–2624. https://doi.org/10.1109/TUFFC.2012.2502.
[12] H. Sato-Akaba, M. Tseytlin, Development of an L-band rapid scan EPR digital console, Journal of Magnetic Resonance 304 (2019). https://doi.org/10.1016/j.jmr.2019.05.003.
[13] H. Sato-Akaba, Y. Okada, K. Tsuji, M.C. Emoto, H.G. Fujii, Design and Fabrication of Compact Arrayed Magnet for Biological EPR Imaging, Appl Magn Reson 52 (2021) 1017–1029. https://doi.org/10.1007/s00723-020-01256-4.
[14] H. Sato-Akaba, Y. Kuwahara, H. Fujii, H. Hirata, Half-life mapping of nitroxyl radicals with three-dimensional electron paramagnetic resonance imaging at an interval of 3.6 seconds., Anal Chem 81 (2009) 7501–6. https://doi.org/10.1021/ac901169g.
[15] R. Nakaoka, K. Kato, K. Yamamoto, H. Yasui, S. Matsumoto, I.A. Kirilyuk, V. V Khramtsov, O. Inanami, H. Hirata, Electron Paramagnetic Resonance Implemented with Multiple Harmonic Detections Successfully Maps Extracellular pH In Vivo, Anal Chem 95 (2023) 3940–3950. https://doi.org/10.1021/acs.analchem.2c03194.
[16] J.S. Hyde, T.G. Camenisch, J.J. Ratke, R.A. Strangeway, W. Froncisz, Digital Detection by Time-Locked Sampling in EPR, Biol Magn Reson 24 (2005) 199–222. https://doi.org/10.1007/0-306-48533-8_7.
[17] M. Tseitlin, R.W. Quine, G.A. Rinard, S.S. Eaton, G.R. Eaton, Digital EPR with an arbitrary waveform generator and direct detection at the carrier frequency, Journal of Magnetic Resonance 213 (2011) 119–125. https://doi.org/10.1016/j.jmr.2011.09.024.
[18] J. Kozioł, P. Rajda, R. Rumian, T. Oleś, P. Budzioch, R.J. Gurbiel, W. Froncisz, Continuous wave electron paramagnetic resonance L-band spectrometer with direct digitalization using time-locked subsampling, Journal of Magnetic Resonance 322 (2021) 106870. https://doi.org/https://doi.org/10.1016/j.jmr.2020.106870.
[19] H. Sato-Akaba, H. Fujii, H. Hirata, Improvement of temporal resolution for three-dimensional continuous-wave electron paramagnetic resonance imaging, Review of Scientific Instruments 79 (2008) 123701. https://doi.org/10.1063/1.3033161.
[20] S.S. Eaton, Y. Shi, L. Woodcock, L.A. Buchanan, J. McPeak, R.W. Quine, G.A. Rinard, B. Epel, H.J. Halpern, G.R. Eaton, Rapid-scan EPR imaging, Journal of Magnetic Resonance 280 (2017) 140–148. https://doi.org/10.1016/j.jmr.2017.02.013.
[21] J.W. Stoner, D. Szymanski, S.S. Eaton, R.W. Quine, G.A. Rinard, G.R. Eaton, Direct-detected rapid-scan EPR at 250MHz, Journal of Magnetic Resonance 170 (2004) 127–135. https://doi.org/https://doi.org/10.1016/j.jmr.2004.06.008.